

<https://doi.org/10.14379/iodp.proc.355.201.2017>

# Data report: $^{87}\text{Sr}/^{86}\text{Sr}$ in pore fluids from IODP Expedition 355 Arabian Sea Monsoon<sup>1</sup>



## Contents

- 1 Abstract
- 1 Introduction
- 2 Analytical methods
- 3 Results and discussion
- 5 Conclusion
- 5 Acknowledgments
- 6 References

Samantha C. Carter,<sup>2</sup> Elizabeth M. Griffith,<sup>2</sup> Howie D. Scher,<sup>3</sup> and the Expedition 355 Scientists<sup>4</sup>

Keywords: International Ocean Discovery Program, IODP, *JOIDES Resolution*, Expedition 355, Site U1456, Site U1457, strontium, pore fluid, Arabian Sea,  $^{87}\text{Sr}/^{86}\text{Sr}$

## Abstract

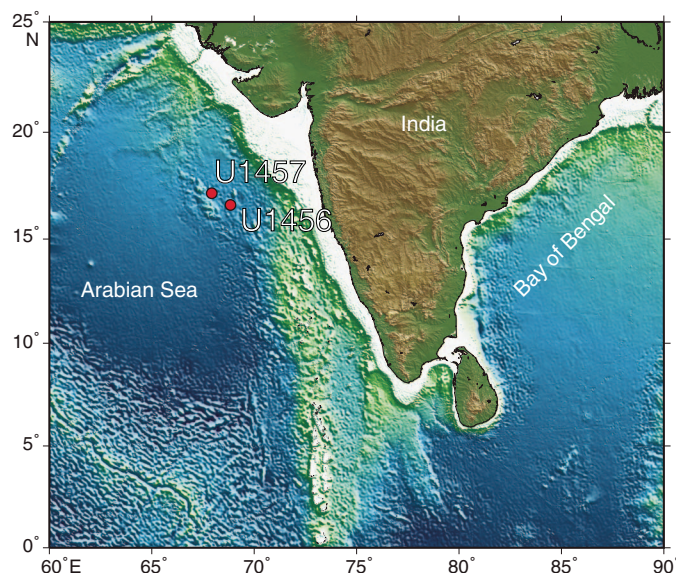
Here we report the strontium isotope ratios ( $^{87}\text{Sr}/^{86}\text{Sr}$ ) from pore fluids collected during International Ocean Discovery Program (IODP) Expedition 355. Ratios from Sites U1456 ( $N = 21$ ) and U1457 ( $N = 20$ ) are reported. Pore fluid  $^{87}\text{Sr}/^{86}\text{Sr}$  is a useful tool to establish fluid-rock reactions, sources of Sr, and fluid mixing. The measured  $^{87}\text{Sr}/^{86}\text{Sr}$  of the pore fluid has significant variations at both sites, and three distinct zones are identified. At Site U1456,  $^{87}\text{Sr}/^{86}\text{Sr}$  starts at values similar to that of modern seawater ( $\sim 0.7092$ ) from near the seafloor down to  $\sim 100$  meters below seafloor (mbsf). Over this interval, Sr concentration increases, whereas Ca decreases (Zone 1). Below 100 mbsf,  $^{87}\text{Sr}/^{86}\text{Sr}$  values increase to a max of  $\sim 0.7100$  at  $\sim 224$  mbsf, and Sr concentrations decrease (Zone 2). Isotopic values then gradually decrease to  $\sim 0.7085$ , with an increase in Sr concentrations (Zone 3). Site U1457 displays the same general trends in pore fluid  $^{87}\text{Sr}/^{86}\text{Sr}$  composition; however, there are distinct differences. First, Zone 1 occurs over a shorter interval ( $\sim 0$ – $54$  mbsf) due to a lower sedimentation rate, and it also has lower Sr concentrations compared to Site U1456. Additionally,  $^{87}\text{Sr}/^{86}\text{Sr}$  reaches a higher peak value in Zone 2 than at Site U1456. Finally, in Zone 3 the maximum Sr concentration reached is significantly lower than that at Site U1456.

## Introduction

International Ocean Discovery Program (IODP) Expedition 355, Arabian Sea Monsoon, was designed to achieve a better understanding of weathering and erosional patterns in the Himalayan region and of how these patterns respond to variations in the intensity of the Asian monsoon (see the [Expedition 355 summary](#) chapter [Pandey et al., 2016b]). To achieve this goal, two sites were drilled, Sites U1456 and U1457 (Figure F1), both located within Laxmi Ba-

sin in the eastern Arabian Sea. Drilling recovered sediments extending back to the middle Miocene at Site U1456. At Site U1457, lower Paleocene sediments were recovered directly overlying the basement rock. Laxmi Basin has a significant amount of sediment cover overlying the basement. Clastic sediments within the Arabian Sea are primarily sourced from the Indus River and its associated tributaries and have been since the onset of the India/Eurasia collision (Clift et al., 2001). These sites were drilled primarily to reveal how the Indus Fan evolved through time, to reconstruct the weathering

Figure F1. Map showing location of Sites U1456 and U1457 (modified from map created by the International Ocean Discovery Program, *JOIDES Resolution* Science Operator).



<sup>1</sup> Carter, S.C., Griffith, E.M., Scher, H.D., and the Expedition 355 Scientists, 2017. Data report:  $^{87}\text{Sr}/^{86}\text{Sr}$  in pore fluids from IODP Expedition 355 Arabian Sea Monsoon. In Pandey, D.K., Clift, P.D., Kulhanek, D.K., and the Expedition 355 Scientists, *Arabian Sea Monsoon*. Proceedings of the International Ocean Discovery Program, 355: College Station, TX (International Ocean Discovery Program). <https://doi.org/10.14379/iodp.proc.355.201.2017>

<sup>2</sup> School of Earth Sciences, The Ohio State University, USA. Correspondence author: [carter.1563@osu.edu](mailto:carter.1563@osu.edu)

<sup>3</sup> Department of Earth and Ocean Sciences, University of South Carolina, USA.

<sup>4</sup> Expedition 355 Scientists addresses.

MS 355-201: Received 26 August 2016 · Accepted 6 July 2017 · Published 24 October 2017

This work is distributed under the [Creative Commons Attribution 4.0 International](#) (CC BY 4.0) license. 

and erosion history of the Western Himalaya, and to address questions pertaining to the nature of the basement in Laxmi Basin (see the [Expedition 355 summary](#) chapter [Pandey et al., 2016b]). The recovered sediment allows for examination of the evolution of the Indus Fan since the late Miocene.

Sediments and pore fluids from these cores will be used by scientists to achieve the scientific objectives of Expedition 355. However, these sediments and pore fluids, and any potential proxies archived within them, may be significantly affected by diagenetic reactions occurring within the sediment after deposition, which may affect the signal that is ultimately recorded. In order to make valid interpretations of any proxy record made using samples from the cores, we must first understand what processes have occurred within the sediment and how these processes may have altered them.

Waters buried with sediments are subject to major compositional changes during diagenesis of the sediments. These pore fluids contain a number of tracers that can be used to identify fluid sources and diagenetic reactions. The strontium isotope composition ( $^{87}\text{Sr}/^{86}\text{Sr}$ ) of pore waters is a conservative tracer that does not undergo biological fractionation (Mook, 2001) and has been useful in establishing fluid-rock reactions, sources of Sr, and fluid mixing (e.g., Torres et al., 2004; Teichert et al., 2005; Solomon et al., 2009; Joseph et al., 2012, 2013; Moen et al., 2015).

There are several possible sources of Sr to pore fluids recovered with buried marine sediments, each with a distinct range of  $^{87}\text{Sr}/^{86}\text{Sr}$  values. The first is coeval seawater, which has  $^{87}\text{Sr}/^{86}\text{Sr}$  values that depend on the age of deposition. Modern seawater has a  $^{87}\text{Sr}/^{86}\text{Sr}$  value of 0.7092 (McArthur et al., 2012). Another possible source is alteration of continental material. The bulk of the continents are enriched in radiogenic  $^{87}\text{Sr}$ , and thus continental felsic and basaltic rocks have relatively high isotopic values ( $^{87}\text{Sr}/^{86}\text{Sr}$  ranges from  $\sim 0.7010$  to  $\sim 0.7180$ ; Faure and Powell, 1972) that, if altered by diagenetic processes, may affect pore fluids. Another possible source is dissolution of biogenic calcite, which has Sr isotopic values ranging from  $\sim 0.7075$  to  $0.7092$  coeval with seawater (100 to 0 Ma) (e.g., Gieskes 1981; Hess et al., 1986; Baker et al., 1982; Fantle and DePaolo, 2006; McArthur et al., 2012). Finally, fluid flow from the oceanic crust ( $\sim 0.703$ ; Veizer, 1989) beneath the sediment may also have an effect on the isotopic composition of the pore fluid near the sediment/crust interface if advection of fluids is significant, which is most common in sediment deposited above very young oceanic crust (Gieskes, 1981; Elderfield and Gieskes, 1982).

This study presents records of  $^{87}\text{Sr}/^{86}\text{Sr}$  from pore fluids recovered from Sites U1456 and U1457 that were drilled as part of Expedition 355. It should be noted that the data reported here extend to a maximum depth of 864 meters below seafloor (mbsf) at Site U1456 and 848 mbsf at Site U1457. Each site has cored sections below the depths of the samples analyzed; however, pore water fluid sampling was discontinued at these depths. As such, there may be processes occurring within the deepest sediments (lithologic Unit V) not included here. The data reported will be useful for future studies using these sediments and pore fluids to examine fluid-rock reactions that have occurred so that researchers may have a better understanding of the diagenetic processes that have affected the sediments and pore fluids.

## Analytical methods

Interstitial waters were extracted on board from 5 to 15 cm long whole-round sections that were cut and capped immediately after core retrieval on deck (see the [Expedition 355 methods](#) chapter [Pandey et al., 2016a]). Whole-round samples were taken at a frequency of one sample per core (every  $\sim 9.5$  m) or every other core when using the half-length advanced piston corer (HLAPC). Before squeezing, samples were removed from the core liner and the outer surface was carefully scraped with a spatula to minimize potential contamination by the coring process. The cleaned whole-round samples were placed into a titanium and steel squeezing device modified after the stainless steel squeezer of Manheim and Sayles (1974) and squeezed at ambient temperature with a hydraulic press at pressures of up to  $\sim 30,000$  psi. The pore water squeezed out of the sediment was extruded into a prewashed (in 10% hydrochloric acid) 60 mL plastic syringe attached to the bottom of the squeezer assembly. The solution was subsequently filtered through a  $0.45\ \mu\text{M}$  polysulfone disposable filter (Whatman) into separate vials.

Calcium ( $\text{Ca}^{2+}$ ) and strontium ( $\text{Sr}^{2+}$ ) concentrations of interstitial waters were measured as part of the suite of shipboard geochemical measurements.  $\text{Ca}^{2+}$  concentrations were measured by ion chromatography, with an analytical percent error within 1.2% (see the [Expedition 355 methods](#) chapter [Pandey et al., 2016a]).  $\text{Sr}^{2+}$  concentrations were measured by inductively coupled plasma-atomic emission spectroscopy (ICP-AES) with an analytical percent error better than 1% (see the [Expedition 355 methods](#) chapter [Pandey et al., 2016a]).

The isotopic composition of Sr was measured on shore after the end of the expedition in pore fluid samples recovered from 2.95 to 863.69 mbsf at Site U1456 ( $N = 21$ ) and from 7.87 to 847.97 mbsf at Site U1457 ( $N = 20$ ). Sr concentrations of from shipboard analyses were used to measure out a specific volume of each pore fluid sample equivalent to  $1\ \mu\text{g}$  of Sr for isotopic analysis. Separation of Sr was carried out in the clean laboratory facility located at the University of Texas at Arlington, following the method outlined by Scher et al. (2014). Samples were heated to evaporation in a chemical fume hood. Dried residues were reconstituted in  $100\ \mu\text{L}$  of 8 M ultrapure  $\text{HNO}_3$  and loaded directly onto Teflon microcolumns with  $125\ \mu\text{L}$  stem volumes loaded with Sr-spec resin (Eichrom Technologies, LLC, USA). After loading the sample onto the resin bed,  $2\ \text{mL}$  of 8 M ultrapure nitric acid was passed through the columns to elute major elements and trace metals. These elutions were discarded. Prewashed Teflon vials were then placed under the columns and  $1\ \text{mL}$   $0.005\ \text{M}$  ultrapure nitric acid was passed through the columns to elute the Sr. Three method blanks were processed in the same manner as described and yielded an average of  $17\ \text{pg}$  of Sr or about  $60,000\times$  lower than the samples.

Isotopic analysis of the solution was carried out using the Neptune Plus multicollector inductively coupled plasma-mass spectrometer (MC-ICPMS) at the University of South Carolina (USA) following Scher et al. (2014). Instrumental mass fractionation during analyses was corrected by normalizing measured ratios to  $^{86}\text{Sr}/^{88}\text{Sr} = 0.1194$  using an exponential law. Replicate analysis of standard reference Material (SRM) 987 yielded  $0.710315 \pm 0.000010$  ( $2\sigma$ ,  $N = 17$ ) for a first set of samples and  $0.710306 \pm 0.000012$  ( $2\sigma$ ,  $N$

Table T1. Isotopic composition of Sr measured in pore fluid samples, Site U1456. Sr and Ca concentrations are from shipboard measurements (see the Site U1456 chapter [Pandey et al., 2016c]). Standard error of the mean (SEM) is the standard deviation of the sample means over all possible samples. 2SEM is 2× SEM, which represents the 95% confidence level. — = measurements not taken. [Download table in CSV format.](#)

Core section	Top interval (cm)	Bottom interval (cm)	Depth (mbsf)	Sr ( $\mu\text{M}$ )	$^{87}\text{Sr}/^{86}\text{Sr}$	2SEM	Ca (mM)
355-U1456A-							
1H-2	145	150	2.95	99.06	0.709228	0.000008	10.031
4H-5	145	150	30.95	81.25	0.709169	0.000010	3.939
7H-5	145	150	59.45	162.71	0.709164	0.000011	3.998
11H-5	145	150	97.45	298.97	0.709157	0.000008	6.071
14H-3	145	150	122.95	202.93	0.709346	0.000007	5.512
17F-3	95	100	142.97	170.37	0.709551	0.000014	7.768
25F-3	145	150	180.56	130.60	0.709980	0.000007	9.270
35F-1	145	150	224.55	123.81	0.709999	0.000008	8.926
42F-2	141	146	256.91	130.82	0.709861	0.000005	8.875
52F-2	145	150	303.15	135.42	0.709634	0.000007	7.448
67F-2	140	150	373.60	149.46	0.709110	0.000006	6.070
355-U1456C-							
41X-2	140	150	430.60	179.89	0.708933	0.000010	9.297
355-U1456D-							
5R-2	94	104	490.04	183.62	0.708733	0.000008	9.521
10R-3	135	145	540.55	181.17	0.708561	0.000009	9.998
18R-1	102	117	615.02	263.11	0.708526	0.000006	13.299
21R-2	115	130	645.75	283.60	0.708519	0.000005	14.427
25R-2	135	150	684.75	300.75	0.708510	0.000015	14.252
29R-2	128	143	723.18	338.62	0.708561	0.000006	12.968
35R-4	107	122	784.47	430.90	0.708563	0.000006	—
37R-3	134	149	802.64	446.62	0.708564	0.000006	15.095
40R-3	88	103	830.93	536.60	0.708550	0.000007	—
43R-6	135	150	863.69	576.15	0.708520	0.000007	—

= 13) for a second set.  $^{87}\text{Sr}/^{86}\text{Sr}$  data were normalized to SRM 987, which has a reported  $^{87}\text{Sr}/^{86}\text{Sr}$  value of 0.710248 (McArthur, 1994). Associated analytical error for each measurement can be found in Tables T1 and T2.

## Results and discussion

### Site U1456

Overall, the Sr isotopic composition of the pore fluid from Site U1456 has significant variations throughout the analyzed cored sections, and there appears to be three distinct zones showing different  $^{87}\text{Sr}/^{86}\text{Sr}$  patterns (Figure F2). In Zone 1, at the top of the site, the pore fluid has  $^{87}\text{Sr}/^{86}\text{Sr}$  values similar to that of modern seawater ( $\sim 0.7092$ ) down to  $\sim 100$  mbsf. Over this depth interval (0–100 mbsf), Sr concentration in the pore fluid increases, whereas Ca decreases. This interval corresponds to lithologic Unit I, which is characterized by nanofossil ooze and foraminifer-rich nanofossil ooze interbedded with clay, silt, and sand (see the Site U1456 chapter [Pandey et al., 2016c]). The carbonate sediments in the top 100 m of the site are all Pleistocene in age or younger. In general, calcareous nanofossils are moderately to well preserved throughout Site U1456, whereas planktonic foraminifer preservation varies from poor to good (see the Site U1456 chapter [Pandey et al., 2016c]).

In Zone 2, below 100 mbsf,  $^{87}\text{Sr}/^{86}\text{Sr}$  values rapidly increase to a maximum value of  $\sim 0.7100$  between 97 and 224 mbsf, whereas Sr concentrations decrease (Figure F2). There are several potential sources of material with high  $^{87}\text{Sr}/^{86}\text{Sr}$  to the Arabian Sea, each with

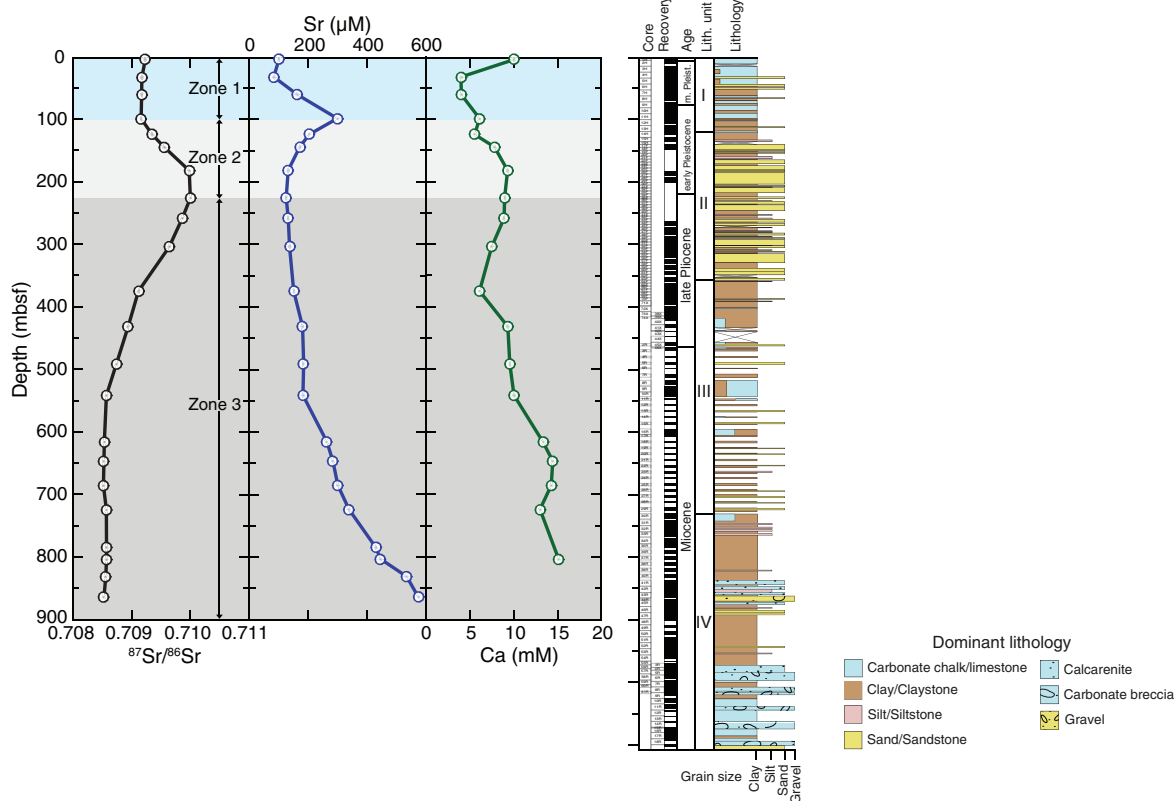
Table T2. Isotopic composition of Sr measured in pore fluid samples, Site U1457. Sr and Ca concentrations are from shipboard measurements (see the Site U1457 chapter [Pandey et al., 2016d]). Standard error of the mean (SEM) is the standard deviation of the sample means over all possible samples. 2SEM is 2× SEM, which represents the 95% confidence level. — = measurements not taken. [Download table in CSV format.](#)

Core section	Top interval (cm)	Bottom interval (cm)	Depth (mbsf)	Sr ( $\mu\text{M}$ )	$^{87}\text{Sr}/^{86}\text{Sr}$	2SEM	Ca (mM)
355-U1457A-							
1H-6	115	120	7.87	120.62	0.709158	0.000009	6.842
3H-5	145	150	25.65	156.44	0.709158	0.000010	4.770
4H-5	145	150	35.15	182.03	0.709182	0.000007	4.694
6H-5	145	150	54.15	206.59	0.709213	0.000006	4.355
8H-5	145	150	73.15	169.62	0.709360	0.000010	4.480
9H-5	145	150	81.06	141.44	0.709511	0.000008	4.971
11H-2	145	150	97.15	115.05	0.709769	0.000009	5.750
355-U1457B-							
19F-2	140	150	137.10	104.15	0.710198	0.000007	7.718
27F-2	110	120	174.32	106.09	0.710304	0.000011	8.236
31F-2	134	144	193.38	113.04	0.710316	0.000007	8.545
355-U1457C-							
9R-2	111	121	262.11	125.62	0.710036	0.000008	9.737
19R-4	140	150	362.40	133.26	0.709614	0.000010	8.071
25R-2	140	150	417.52	134.13	0.709097	0.000007	7.458
33R-2	140	150	495.20	147.75	0.708985	0.000008	9.418
39R-2	140	150	553.40	175.17	0.708838	0.000009	10.234
45R-5	75	85	615.15	195.36	0.708688	0.000006	—
49R-4	135	150	653.35	217.34	0.708614	0.000008	13.392
58R-3	91	106	738.29	204.17	0.708481	0.000010	15.477
66R-2	121	136	814.82	220.78	0.708433	0.000007	14.467
69R-5	136	148	847.97	187.33	0.708499	0.000010	—

distinct typical Sr isotopic compositions. These are continental sources including the Deccan basalts (0.704–0.716; Peng et al., 1998), the higher Himalayan crystalline (0.710–0.908; Oliver et al., 2003; Bickle et al., 2005), the lesser Himalayan silicates (0.706–1.311; Singh et al., 1998; Bickle et al., 2001), the Vindhyan Supergroup (0.705–0.709; Ray et al., 2002; Kumar et al., 2002), and the Peninsular gneisses (0.702–0.725; Peucat et al., 1989). A change in lithology is also seen between Zones 1 and 2, where previously carbonate-rich sediments give way to sediments largely dominated by sand and clay.

In Zone 3, between  $\sim 224$  and  $\sim 540$  mbsf,  $^{87}\text{Sr}/^{86}\text{Sr}$  values decrease gradually to  $\sim 0.7085$ . Below this,  $^{87}\text{Sr}/^{86}\text{Sr}$  values remain relatively constant around 0.7085 over the remainder of the analyzed core samples to 864 mbsf (Figure F2). Also occurring over this interval is a gradual increase in both Sr and Ca concentrations, which reach maximum concentrations of 576  $\mu\text{M}$  (863.69 mbsf) and 15 mM (802.64 mbsf), respectively. Recycled Paleogene carbonates are common throughout this section, where there is evidence of a mass transport deposit (see the Site U1456 chapter [Pandey et al., 2016c]). Marine carbonates from the Paleogene reflect the Sr isotopic signature of coeval seawater, which was less radiogenic than seawater from the late Miocene, which is the maximum age of the sediments examined (see the Site U1456 chapter [Pandey et al., 2016c]). Late Miocene seawater is characterized by  $^{87}\text{Sr}/^{86}\text{Sr}$  values greater than 0.7088 (see McArthur et al., 2012, and references therein). The Sr isotopic composition of carbonates from the Paleogene ranged from  $\sim 0.70820$  in the latest Paleogene (23.03 Ma) to a minimum of 0.70772 in the Ypresian (51 Ma) (see McArthur et al., 2012, and references therein).

Figure F2. Downhole profiles of  $^{87}\text{Sr}/^{86}\text{Sr}$  ratios (this study) and Sr and Ca concentrations (see the Site U1456 chapter [Pandey et al., 2016c]) in pore fluids from Site U1456 in the context of sediment lithology (column from the Site U1456 chapter [Pandey et al., 2016c]). Zones delineate different trends in downhole Sr isotopic composition of pore waters.



### Site U1457

Similar to Site U1456, Site U1457 displays the same general trends in pore fluid  $^{87}\text{Sr}/^{86}\text{Sr}$  composition with depth (Figure F3). However, there are some distinct differences that we highlight. The topmost section (Zone 1) has pore fluid with  $^{87}\text{Sr}/^{86}\text{Sr}$  values similar to that of modern seawater ( $\sim 0.7092$ ), down to  $\sim 54$  mbsf, below which  $^{87}\text{Sr}/^{86}\text{Sr}$  shifts to higher values. This trend is also seen at Site U1456, as both sites are dominated by biogenic calcite in the topmost sections, corresponding to lithologic Unit I. However, the sedimentation rate at Site U1457 was lower ( $\sim 7$  cm/ky) compared to Site U1456 ( $\sim 12$  cm/ky) over this interval (see the [Site U1456](#) and [Site U1457](#) chapters [Pandey et al., 2016c, 2016d]), causing the shift to higher values to begin at a shallower depth at Site U1457 ( $\sim 54$  mbsf) compared to Site U1456 ( $\sim 100$  mbsf) (Figure F4). Also, at Site U1457 the highest Sr concentration reached over this interval is  $\sim 206$   $\mu\text{M}$ , whereas Sr concentration reaches  $\sim 300$   $\mu\text{M}$  at Site U1456.

Below 54 mbsf (Zone 2),  $^{87}\text{Sr}/^{86}\text{Sr}$  values rapidly increase to a maximum value of  $\sim 0.7103$  at  $\sim 193$  mbsf, whereas Sr concentration decreases (Figure F3). However, the maximum  $^{87}\text{Sr}/^{86}\text{Sr}$  value at Site U1457 is significantly higher than that at Site U1456 ( $0.71032$  compared to  $0.71000$ ) (Figure F4).

Between  $\sim 193$  and  $\sim 615$  mbsf (in Zone 3),  $^{87}\text{Sr}/^{86}\text{Sr}$  values decrease gradually to  $\sim 0.7085$ . Below this,  $^{87}\text{Sr}/^{86}\text{Sr}$  remains relatively constant around  $0.7085$  for the remainder of the analyzed core samples to 848 mbsf (Figure F3). There is also a gradual increase in both Sr and Ca concentrations, which reach maximum concentrations of  $220$   $\mu\text{M}$  ( $814.82$  mbsf) and  $15$  mM ( $738.29$  mbsf), respectively. Reworked Cretaceous and Paleogene nannofossils are also common through this interval at Site U1457 (see the [Site U1457](#) chapter [Pandey et al., 2016d]). However, the maximum Sr concentration reached at Site U1457 ( $220$   $\mu\text{M}$ ) is significantly lower than the maximum Sr concentration reached at Site U1456 ( $576$   $\mu\text{M}$ ) (Figure F4).

Figure F3. Downhole profiles of <sup>87</sup>Sr/<sup>86</sup>Sr ratios (this study) and Sr and Ca concentrations (see the Site U1457 chapter [Pandey et al., 2016d]) in pore fluids from Site U1457 in the context of sediment lithology (column from the Site U1457 chapter [Pandey et al., 2016d]). Zones delineate different trends in downhole Sr isotopic composition of pore waters.

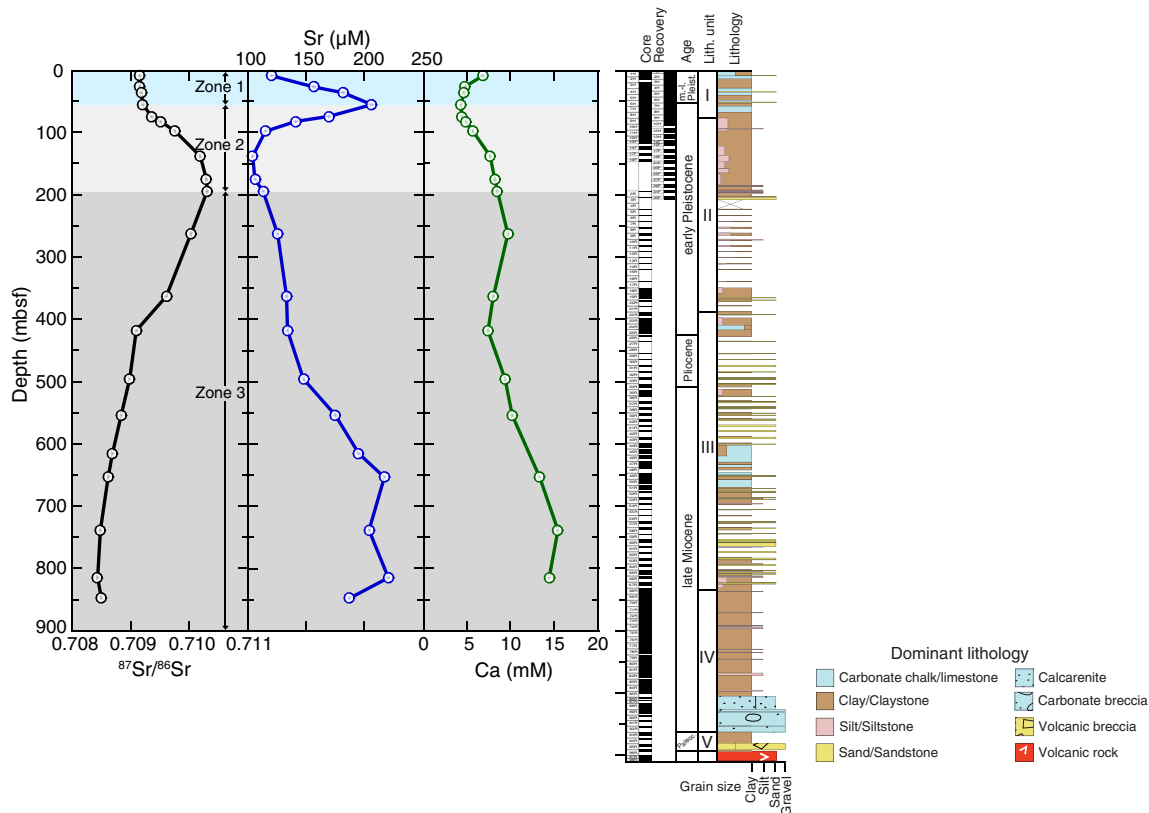
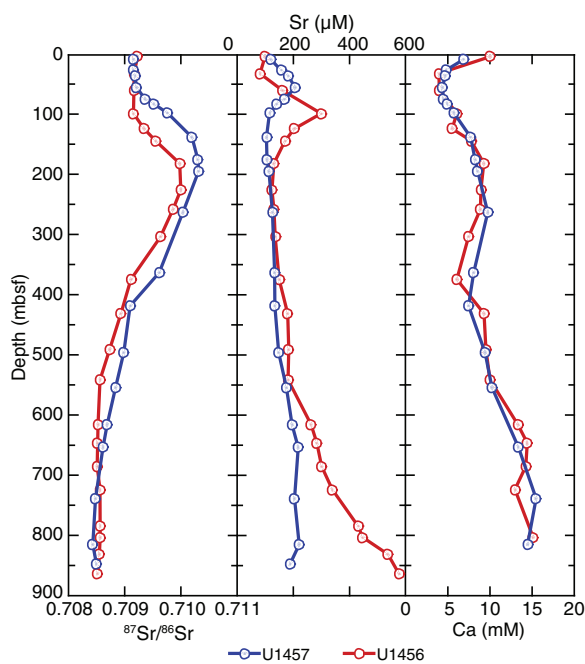


Figure F4. Comparisons of downhole profiles of <sup>87</sup>Sr/<sup>86</sup>Sr ratios (this study) and Sr and Ca concentrations (see the Site U1456 and Site U1457 chapters [Pandey et al., 2016c, 2016d]) in pore fluids between Sites U1456 and U1457.



## Conclusion

According to the data reported here, there are three distinct zones at both sites where different trends of <sup>87</sup>Sr/<sup>86</sup>Sr values (and Sr concentrations) are displayed within the pore fluids. The first, uppermost Zone 1 (~0–100 mbsf at Site U1456 and ~0–54 mbsf at Site U1457), which falls within lithologic Unit I, is identified by pore fluid <sup>87</sup>Sr/<sup>86</sup>Sr values similar to that of modern seawater, increasing Sr concentrations, and decreasing Ca concentrations. Zone 2 (~100–224 mbsf at Site U1456 and ~45–193 mbsf at Site U1457) is characterized by a rapid increase in <sup>87</sup>Sr/<sup>86</sup>Sr values of the pore fluid and a decrease in Sr concentration, dominantly in lithologic Unit II. Finally, Zone 3 (~224–864 mbsf at Site U1456 and ~193–848 mbsf at Site U1457) has gradually decreasing <sup>87</sup>Sr/<sup>86</sup>Sr values until a value of ~0.7085 is reached, where it remains relatively constant. This interval corresponds to lithologic Units III and IV (the latter was only measured at Site U1456).

## Acknowledgments

This research used samples and data provided by the International Ocean Discovery Program (IODP). Funding for this research was provided by a U.S. Science Support Program Post-Expedition Activity Award to E.M. Griffith. We thank Cédric M. John and Denise K. Kulhanek for providing important comments, which helped to improve the present manuscript.

## References

- Baker, P.A., Gieskes, J.M., and Elderfield, H., 1982. Diagenesis of carbonates in deep-sea sediments: evidence from Sr/Ca ratios and interstitial dissolved Sr<sup>2+</sup> data. *Journal of Sedimentary Research*, 52(1):71–82. <https://doi.org/10.1306/212F7EE1-2B24-11D7-8648000102C1865D>
- Bickle, M.J., Chapman, H.J., Bunbury, J., Harris, N.B.W., Fairchild, I.J., Ahmad, T., and Pomiés, C., 2005. Relative contributions of silicate and carbonate rocks to riverine Sr fluxes in the headwaters of the Ganges. *Geochimica et Cosmochimica Acta*, 69(9):2221–2240. <https://doi.org/10.1016/j.gca.2004.11.019>
- Bickle, M.J., Harris, N.B.W., Bunbury, J.M., Chapman, H.J., Fairchild, I.J., and Ahmad, T., 2001. Controls on the <sup>87</sup>Sr/<sup>86</sup>Sr ratio of carbonates in the Garhwal Himalaya, headwaters of the Ganges. *Journal of Geology*, 109(6):737–753. <https://doi.org/10.1086/323192>
- Clift, P.D., Shimizu, N., Layne, G.D., Blusztajn, J.S., Gaedicke, C., Schlüter, H.-U., Clark, M.K., and Amjad, S., 2001. Development of the Indus Fan and its significance for the erosional history of the western Himalaya and Karakoram. *Geological Society of America Bulletin*, 113(8):1039–1051. [https://doi.org/10.1130/0016-7606\(2001\)113<1039:DOT-IFA>2.0.CO;2](https://doi.org/10.1130/0016-7606(2001)113<1039:DOT-IFA>2.0.CO;2)
- Elderfield, H., and Gieskes, J.M., 1982. Sr isotopes in interstitial waters of marine sediments from Deep Sea Drilling Project cores. *Nature*, 300(5892):493–497. <https://doi.org/10.1038/300493a0>
- Fantle, M.S., and DePaolo, D.J., 2006. Sr isotopes and pore fluid chemistry in carbonate sediment of the Ontong Java Plateau: calcite recrystallization rates and evidence for a rapid rise in seawater Mg over the last 10 million years. *Geochimica et Cosmochimica Acta*, 70(15):3883–3904. <https://doi.org/10.1016/j.gca.2006.06.009>
- Faure, G., and Powell, J.L., 1972. *Strontium Isotope Geology*: New York (Springer-Verlag). <https://doi.org/10.1007/978-3-642-65367-4>
- Gieskes, J.M., 1981. Deep-sea drilling interstitial water studies: implications for chemical alteration of the oceanic crust, Layers I and II. In Warme, J.E., Douglas, R.G., and Winterer, E.L. (Eds.), *The Deep Sea Drilling Project: A Decade of Progress*. Special Publication - Society of Economic Paleontologists and Mineralogists, 32:149–167. [http://archives.datapages.com/data/sepm\\_sp/SP32/Deep\\_Sea\\_Drilling\\_Interstitial\\_Water\\_Studies.html](http://archives.datapages.com/data/sepm_sp/SP32/Deep_Sea_Drilling_Interstitial_Water_Studies.html)
- Hess, J., Bender, M.L., and Schilling, J.-G., 1986. Evolution of the ratio of strontium-87 to strontium-86 in seawater from Cretaceous to present. *Science*, 231(4741):979–984. <https://doi.org/10.1126/science.231.4741.979>
- Joseph, C., Torres, M.E., and Haley, B., 2013. Data report: <sup>87</sup>Sr/<sup>86</sup>Sr in pore fluids from NanTroSEIZE Expeditions 322 and 333. In Saito, S., Underwood, M.B., Kubo, Y., and the Expedition 322 Scientists, *Proceedings of the Integrated Ocean Drilling Program*, 322: Tokyo (Integrated Ocean Drilling Program Management International, Inc.). <https://doi.org/10.2204/iodp.proc.322.207.2013>
- Joseph, C., Torres, M.E., Martin, R.A., Haley, B.A., Pohlman, J.W., Riedel, M., and Rose, K., 2012. Using the <sup>87</sup>Sr/<sup>86</sup>Sr of modern and paleoseep carbonates from northern Cascadia to link modern fluid flow to the past. *Chemical Geology*, 334:122–130. <https://doi.org/10.1016/j.chemgeo.2012.10.020>
- Kumar, B., Das Sharma, S., Sreenivas, B., Dayal, A.M., Rao, M.N., Dubey, N., and Chawla, B.R., 2002. Carbon, oxygen and strontium isotope geochemistry of Proterozoic carbonate rocks of the Vindhyan Basin, central India. *Precambrian Research*, 113(1–2):43–63. [https://doi.org/10.1016/S0301-9268\(01\)00199-1](https://doi.org/10.1016/S0301-9268(01)00199-1)
- Manheim, F.T., and Sayles, F.L., 1974. Composition and origin of interstitial waters of marine sediments, based on deep sea drill cores. In Goldberg, E.D. (Ed.), *The Sea* (Volume 5): *Marine Chemistry: The Sedimentary Cycle*: New York (Wiley), 527–568.
- McArthur, J.M., 1994. Recent trends in strontium isotope stratigraphy. *Terra Nova*, 6(4):331–358. <https://doi.org/10.1111/j.1365-3121.1994.tb00507.x>
- McArthur, J.M., Howarth, R.J., and Shields, G.A., 2012. Strontium isotope stratigraphy. In Gradstein, F.M., Schmitz, J.G.O.D., and Ogg, G.M. (Eds.), *The Geologic Time Scale*: Boston (Elsevier), 127–144. <https://doi.org/10.1016/B978-0-444-59425-9.00007-X>
- Moen, N., Hong, W.-L., and Haley, B., 2015. Data report: <sup>87</sup>Sr/<sup>86</sup>Sr in pore fluids off Shimokita, Japan. In Inagaki, F., Hinrichs, K.-U., Kubo, Y., and the Expedition 337 Scientists, *Proceedings of the Integrated Ocean Drilling Program*, 337: Tokyo (Integrated Ocean Drilling Program Management International, Inc.). <https://doi.org/10.2204/iodp.proc.337.201.2015>
- Mook, W.G., 2001. Applications to low-temperature systems. In Geyh, M. (Ed.), *Environmental Isotopes in the Hydrological Cycle: Principles and Applications* (Volume 4): *Groundwater: Saturated and Unsaturated Zone*: Vienna (International Atomic Energy Agency), 349–387. [http://www-naweb.iaea.org/napc/ih/documents/global\\_cycle/vol%20IV/IV\\_Ch5.pdf](http://www-naweb.iaea.org/napc/ih/documents/global_cycle/vol%20IV/IV_Ch5.pdf)
- Oliver, L., Harris, N., Bickle, M., Chapman, H., Dise, N., and Horstwood, M., 2003. Silicate weathering rates decoupled from the <sup>87</sup>Sr/<sup>86</sup>Sr ratio of the dissolved load during Himalayan erosion. *Chemical Geology*, 201(1–2):119–139. [https://doi.org/10.1016/S0009-2541\(03\)00236-5](https://doi.org/10.1016/S0009-2541(03)00236-5)
- Pandey, D.K., Clift, P.D., Kulhanek, D.K., Andò, S., Bendle, J.A.P., Bratenkov, S., Griffith, E.M., Gurumurthy, G.P., Hahn, A., Iwai, M., Khim, B.-K., Kumar, A., Kumar, A.G., Liddy, H.M., Lu, H., Lyle, M.W., Mishra, R., Radhakrishna, T., Routledge, C.M., Saraswat, R., Saxena, R., Scardia, G., Sharma, G.K., Singh, A.D., Steinke, S., Suzuki, K., Tauxe, L., Tiwari, M., Xu, Z., and Yu, Z., 2016a. Expedition 355 methods. In Pandey, D.K., Clift, P.D., Kulhanek, D.K., and the Expedition 355 Scientists, *Arabian Sea Monsoon*. Proceedings of the International Ocean Discovery Program, 355: College Station, TX (International Ocean Discovery Program). <https://doi.org/10.14379/iodp.proc.355.102.2016>
- Pandey, D.K., Clift, P.D., Kulhanek, D.K., Andò, S., Bendle, J.A.P., Bratenkov, S., Griffith, E.M., Gurumurthy, G.P., Hahn, A., Iwai, M., Khim, B.-K., Kumar, A., Kumar, A.G., Liddy, H.M., Lu, H., Lyle, M.W., Mishra, R., Radhakrishna, T., Routledge, C.M., Saraswat, R., Saxena, R., Scardia, G., Sharma, G.K., Singh, A.D., Steinke, S., Suzuki, K., Tauxe, L., Tiwari, M., Xu, Z., and Yu, Z., 2016b. Expedition 355 summary. In Pandey, D.K., Clift, P.D., Kulhanek, D.K., and the Expedition 355 Scientists, *Arabian Sea Monsoon*. Proceedings of the International Ocean Discovery Program, 355: College Station, TX (International Ocean Discovery Program). <https://doi.org/10.14379/iodp.proc.355.101.2016>
- Pandey, D.K., Clift, P.D., Kulhanek, D.K., Andò, S., Bendle, J.A.P., Bratenkov, S., Griffith, E.M., Gurumurthy, G.P., Hahn, A., Iwai, M., Khim, B.-K., Kumar, A., Kumar, A.G., Liddy, H.M., Lu, H., Lyle, M.W., Mishra, R., Radhakrishna, T., Routledge, C.M., Saraswat, R., Saxena, R., Scardia, G., Sharma, G.K., Singh, A.D., Steinke, S., Suzuki, K., Tauxe, L., Tiwari, M., Xu, Z., and Yu, Z., 2016c. Site U1456. In Pandey, D.K., Clift, P.D., Kulhanek, D.K., and the Expedition 355 Scientists, *Arabian Sea Monsoon*. Proceedings of the International Ocean Discovery Program, 355: College Station, TX (International Ocean Discovery Program). <https://doi.org/10.14379/iodp.proc.355.103.2016>
- Pandey, D.K., Clift, P.D., Kulhanek, D.K., Andò, S., Bendle, J.A.P., Bratenkov, S., Griffith, E.M., Gurumurthy, G.P., Hahn, A., Iwai, M., Khim, B.-K., Kumar, A., Kumar, A.G., Liddy, H.M., Lu, H., Lyle, M.W., Mishra, R., Radhakrishna, T., Routledge, C.M., Saraswat, R., Saxena, R., Scardia, G., Sharma, G.K., Singh, A.D., Steinke, S., Suzuki, K., Tauxe, L., Tiwari, M., Xu, Z., and Yu, Z., 2016d. Site U1457. In Pandey, D.K., Clift, P.D., Kulhanek, D.K., and the Expedition 355 Scientists, *Arabian Sea Monsoon*. Proceedings of the International Ocean Discovery Program, 355: College Station, TX (International Ocean Discovery Program). <https://doi.org/10.14379/iodp.proc.355.104.2016>
- Peng, Z.X., Mahoney, J.J., Hooper, P.R., Macdougall, J.D., and Krishnamurthy P., 1998. Basalts of the northeastern Deccan Traps, India: isotopic and elemental geochemistry and relation to southwestern Deccan stratigraphy. *Journal of Geophysical Research: Solid Earth*, 103(B12):29843–29865. <https://doi.org/10.1029/98JB01514>
- Peucat, J.J., Vidal, P., Bernard-Griffiths, J., and Condie, K.C., 1989. Sr, Nd, and Pb isotopic systematics in the Archean low- to high-grade transition zone

- of southern India: syn-accretion vs. post-accretion granulites. *Journal of Geology*, 97(5):537–549. <https://doi.org/10.1086/629333>
- Ray, J.S., Martin, M.W., Veizer, J., and Bowring, S.A., 2002. U-Pb zircon dating and Sr isotope systematics of the Vindhyan Supergroup, India. *Geology*, 30(2):131–134. [https://doi.org/10.1130/0091-7613\(2002\)030<0131:UPZDAS>2.0.CO;2](https://doi.org/10.1130/0091-7613(2002)030<0131:UPZDAS>2.0.CO;2)
- Scher, H.D., Griffith, E.M., and Buckley, W.P., Jr., 2014. Accuracy and precision of  $^{88}\text{Sr}/^{86}\text{Sr}$  and  $^{87}\text{Sr}/^{86}\text{Sr}$  measurements by MC-ICPMS compromised by high barium concentrations. *Geochemistry, Geophysics, Geosystems*, 15(2): 499–508. <https://doi.org/10.1002/2013GC005134>
- Singh, S.K., Trivedi, J.R., Pande, K., Ramesh, R., and Krishnaswami, S., 1998. Chemical and strontium, oxygen, and carbon isotopic compositions of carbonates from the lesser Himalaya: implications to the strontium isotope composition of the source waters of the Ganga, Ghaghara, and the Indus Rivers. *Geochimica et Cosmochimica Acta*, 62(5):743–755. [https://doi.org/10.1016/S0016-7037\(97\)00381-5](https://doi.org/10.1016/S0016-7037(97)00381-5)
- Solomon, E.A., Kastner, M., Wheat, C.G., Jannasch, H., Robertson, G., Davis, E.E., and Morris, J.D., 2009. Long-term hydrogeochemical records in the oceanic basement and forearc prism at the Costa Rica subduction zone. *Earth and Planetary Science Letters*, 282(1–4):240–251. <https://doi.org/10.1016/j.epsl.2009.03.022>
- Teichert, B.M.A., Torres, M.E., Bohrmann, G., and Eisenhauer, A., 2005. Fluid sources, fluid pathways and diagenetic reactions across an accretionary prism revealed by Sr and B geochemistry. *Earth and Planetary Science Letters*, 239(1–2):106–121. <https://doi.org/10.1016/j.epsl.2005.08.002>
- Torres, M.E., Teichert, B.M.A., Tréhu, A.M., Borowski, W., and Tomaru, H., 2004. Relationship of pore water freshening to accretionary processes in the Cascadia margin: fluid sources and gas hydrate abundance. *Geophysical Research Letters*, 31:L22305. <https://doi.org/10.1029/2004GL021219>
- Veizer, J., 1989. Strontium isotopes in seawater through time. *Annual Review of Earth and Planetary Sciences*, 17(1):141–167. <https://doi.org/10.1146/annurev.earth.17.050189.001041>